

HexaGen3D: StableDiffusion is just one step away from Fast and Diverse Text-to-3D Generation

Antoine Mercier Ramin Nakhli* Mahesh Reddy Rajeev Yasarla
Hong Cai Fatih Porikli Guillaume Berger
Qualcomm AI Research[†]

{amercier, mahkri, ryasarla, hongcai, fporikli, guilberg}@qti.qualcomm.com



Figure 1. HexaGen3D leverages pretrained text-to-image models to generate high-quality textured meshes in 7 seconds. Our approach works well with a broad range of text prompts and generalize to new objects or object compositions not encountered during finetuning.

Abstract

Despite the latest remarkable advances in generative modeling, efficient generation of high-quality 3D assets from textual prompts remains a difficult task. A key challenge lies in data scarcity: the most extensive 3D datasets encompass merely millions of assets, while their 2D counterparts contain billions of text-image pairs. To address this, we propose a novel approach which har-

nesses the power of large, pretrained 2D diffusion models. More specifically, our approach, HexaGen3D, finetunes a pretrained text-to-image model to jointly predict 6 orthographic projections and the corresponding latent tri-plane. We then decode these latents to generate a textured mesh. HexaGen3D does not require per-sample optimization, and can infer high-quality and diverse objects from textual prompts in 7 seconds, offering significantly better quality-to-latency trade-offs when comparing to existing approaches. Furthermore, HexaGen3D demonstrates strong generalization to new objects or compositions.

*Work done at Qualcomm AI Research during an internship.

[†]Qualcomm AI Research is an initiative of Qualcomm Technologies, Inc.

1. Introduction

The creation of 3D assets, crucial across various domains such as gaming, AR/VR, graphic design, anime, and movies, is notably laborious and time-consuming. Despite the use of machine learning techniques to aid 3D artists in some aspects of the task, the development of efficient end-to-end 3D asset generation remains challenging, primarily bottlenecked by the limited availability of high-quality 3D data.

In contrast, image generation has recently witnessed a surge in quality and diversity, driven by the training of large models [14, 31, 34, 36, 37, 48] on large datasets like LAION-5B [38] containing billions of text-image pairs. This progress in 2D generative modeling, coupled with the lack of curated 3D data, has prompted recent efforts to adapt 2D pre-trained models for 3D asset creation. One notable example is DreamFusion [32], which utilizes the prior knowledge of a large 2D diffusion model to guide the optimization of a 3D representation, usually a NeRF [27]. While this approach, dubbed Score Distillation Sampling (SDS), and follow-up variants have showed promising results, their main limitation remains the extremely long generation time, taking anywhere from 20 minutes to several hours, and the lack of diversity across seeds.

To address these challenges, we present HexaGen3D, a novel text-to-3D model that significantly reduces generation time without sacrificing quality or diversity. Similar to DreamFusion, we build upon pre-trained 2D models but instead propose to modify and finetune them for direct, feed-forward, generation of 3D objects. Below are the key contributions of our work:

- We adopt a similar approach to 3DGen [11], but replace their custom-designed latent generative model with a pre-trained text-to-image model, reducing the need for extensive 3D finetuning data and enabling generalization to new objects or compositions not encountered during training.
- We introduce “Orthographic Hexaview guidance”, a novel technique to align the model’s 2D prior knowledge with 3D spatial reasoning. This intermediary task involves predicting six-sided orthographic projections which we then map to our final 3D representation. This allows the U-Net of existing 2D diffusion models to efficiently perform multi-view prediction and 3D asset generation in a sequential manner, with 3D generation only requiring one additional U-Net inference step.
- HexaGen3D competes favorably with existing approaches in quality while taking only seven seconds on an A100 to generate a new object. This speed is orders of magnitude faster than existing approaches based on SDS optimization.

2. Related Work

Recent methods heavily leverage diffusion models [12] for generating 3D meshes from single images and/or textual prompts. In this section, we briefly review these works and refer readers to [30] for a more comprehensive survey.

Using Score Distillation Sampling: Pioneering works, such as DreamFusion [32] and Latent-NeRF [26] generate 3D by training a NeRF using Score Distillation Sampling (SDS). However, they require lengthy, per-sample optimization, taking ~ 2 hours to generate an object. Later methods accelerate this process by first producing a coarse NeRF model and then upscaling or enhancing it, e.g., Magic3D [17], Make-it-3D [42], or by first generating geometry and then baking the texture using images generated from diffusion [43]. These techniques considerably reduce generation time, e.g., to 20 - 40 minutes. More recently, MVDream [40] replaces the guidance model with a multi-view diffusion model, leading to improved visual quality, at the cost of slower generation times, taking up to 3 hours to generate an object. ATT3D [22] proposes to map text prompts to a NeRF embedding using a network. This enables generating a mesh within a second, but lacks mesh quality and generalizability.

Feedforward Generation via Diffusion: Several works use diffusion to directly generate 3D structure or representation [6, 11, 15, 22, 23, 29, 41, 49, 50]. Point-E [29] uses diffusion to generate a point cloud, conditioning on an image synthesized from a text input. Shap-E [13] uses a similar transformer-based diffusion architecture but generates parameters of implicit 3D functions like NeRF or DM Tet. More recently, 3DGen [11] adopts a latent triplane representation, which can be denoised by a diffusion model and fed to a point cloud VAE decoder to generate a 3D mesh. SSD-NeRF [6] also adopts the triplane representation but uses a NeRF decoder.

Leveraging 2D View Synthesis: These works utilize diffusion models to generate new 2D views to support 3D generation. 3DiM [46] generates multiple views of target poses, based on a source view and its pose. One-2-3-45 [18] utilizes Zero-1-to-3 [19] to generate several views of an object. It then constructs a volumetric representation based on the generated images and can produce a mesh within 45 seconds. However, the 2D views are generated one at a time and may not provide consistent multi-view information for the volume. Other works employ diffusion to generate multiple views simultaneously, e.g., SyncDreamer [20], and Instant3D [1], and reconstructs 3D objects based on these synthesized views. Wonder3D [21] creates a multi-domain diffusion model to generate both 2D images and normal maps, and trains a signed distance function to extract the underlying textured mesh. Some papers further introduce 3D awareness into the image synthesis process, e.g., GeNVS [4], NerfDiff [9], SparseFusion [51],

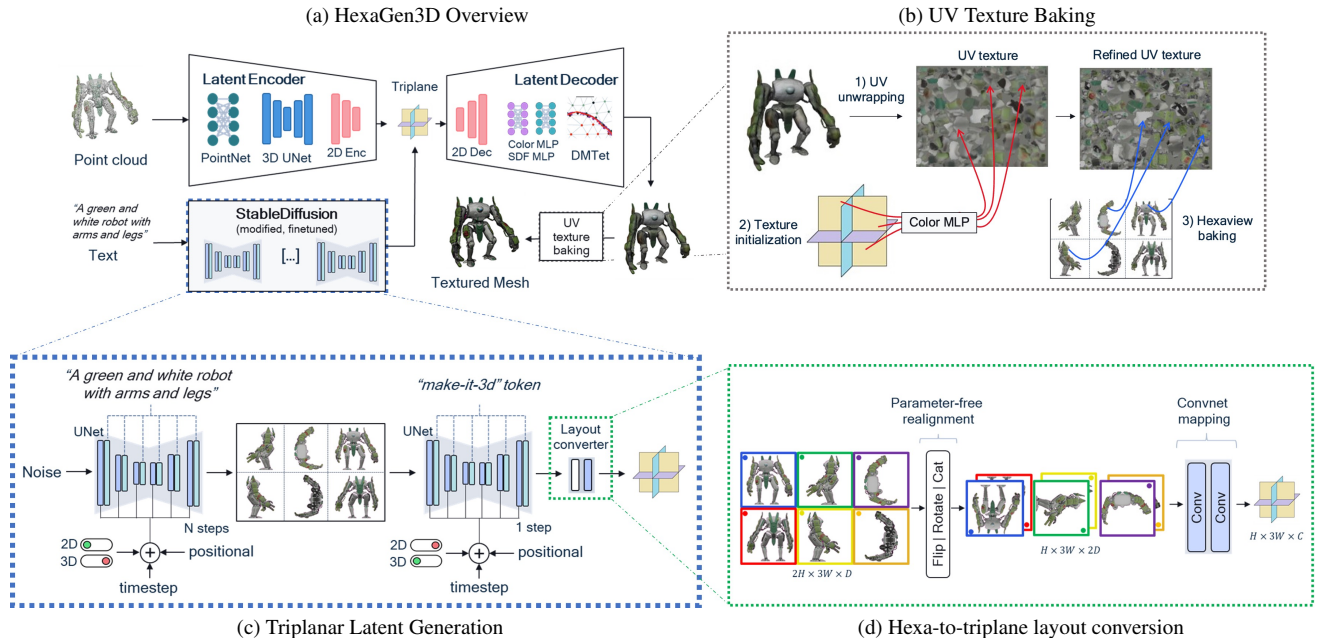


Figure 2. Method overview. HexaGen3D predicts textured meshes from textual prompts in 7 seconds, leveraging pre-trained text-to-image models for latent generation. Like 3DGen [11], the training procedure comprises two stages and the latent representation is based on triplanes. Top-left (a): High-level overview of the two stages: triplanar latent auto-encoder and StableDiffusion-based latent generation. Bottom-left (c): StableDiffusion-based triplanar latent generation via orthographic hexaview diffusion (section 3.2). Bottom-right (d): Detailed overview of our hexa-to-triplane layout converter (section 3.2.3). Top-right (b): Detailed overview of our UV texture baking procedure, used as a post-processing step to improve the visual appearance of the decoded mesh (section 3.3).

Sparse3D [52], providing better multi-view consistency.

Texture Baking: While some of the aforementioned works can also be used to refine textures of an existing mesh [17, 32], several studies focus on texture baking. For instance, Text2Tex [5] and TEXTure [35] uses off-the-shelf StableDiffusion models [36] to iteratively paint texture over known geometry. X-Mesh [25] adopts a dynamic attention module and the CLIP loss between the text prompt and rendered images to generate texture. TexFusion [3] applies a diffusion model’s denoiser on rendered 2D images and aggregates the denoising predictions on a shared latent texture map to achieve better texture consistency.

3. Method

Our latent generative approach, HexaGen3D, leverages pre-trained text-to-image models to predict textured meshes from textual prompts. Like 3DGen [11], the training procedure comprises two stages. In the first stage, we learn a triplanar representation — capturing the shape and color of a textured mesh — using a variational auto-encoder (VAE) [16]. In the second stage, we finetune a pre-trained text-to-image model to synthesize new samples in this triplanar latent space. Figure 2a provides a comprehensive overview of each component.

At test time, we infer new 3D assets in a feedforward manner — without requiring per-sample optimization — allowing for faster and more efficient generation. We first produce triplanar latents from random noise using our latent generator and then convert these latents into a textured mesh using the decoder from the first stage.

For stage 1, our approach retains most architecture components of the auto-encoder from 3DGen [11] (detailed in section 3.1). However, a key distinction of our work is that we propose to leverage pre-trained text-to-image models for stage 2 (detailed in section 3.2). Notably, our results demonstrate that, with proper guidance and minimal finetuning data, 2D generative models such as StableDiffusion transfer surprisingly well to 3D asset generation.

3.1. Stage 1: Learning the Triplanar Representation

In this stage, we train a VAE to learn a triplanar latent representation of textured meshes, derived from point clouds. Our solution closely follows the framework established by 3DGen [11], as we re-use several components from their methodology. Initially, a PointNet model [33] encodes the input point cloud into a triplanar representation. These latents are subsequently refined through two successive networks, and then converted into a textured mesh using a decoder based on the DMTet algorithm [39], as de-

pictured in Figure 2a.

Similar to 3DGen, our pipeline utilizes a U-Net with 3D-aware convs [45] for the first refinement network. However, for the second network, we replace the 3D-aware U-Net architecture used in 3DGen to the VAE architecture typically used in StableDiffusion models [36] and utilize the low-resolution intermediate features from this second network as the target representation for latent generation.

3.2. Stage 2: Triplanar Latent Generation using Pretrained 2D Diffusion Models

In this stage, our goal is to generate triplanar latents that are consistent with the provided textual prompt. Unlike approaches such as 3DGen [11] or Shap-E [13] which focus on developing and training novel architectures from scratch, we aim to build upon pre-trained text-to-image models and explore how to extend them to the 3D domain. A key aspect of our approach is the introduction of a novel intermediary task, “Orthographic Hexaview” prediction, specifically designed to bridge the gap between 2D and 3D synthesis.

3.2.1 Orthographic Hexaview Guidance

As typically done in the literature, our triplanar representation consists of three feature maps concatenated along the width axis to form a 1×3 “rolled-out” layout. This two-dimensional arrangement makes it possible to apply 2D architectures to triplanar latent generation, yet this task still requires 3D geometric reasoning capabilities to ensure feature consistency across the three planes. Our results suggest that pre-trained text-to-image models, despite their prior knowledge on how to arrange multiple objects coherently, struggle when directly fine-tuned to generate such rolled-out triplanes, potentially due to the limited 3D data available during fine-tuning. To address this, we decompose the generation process into two steps, introducing an intermediate “hexaview” representation designed to guide the latent generation process.

As depicted in Fig. 2c, the intermediate “hexaview” representation includes latent features from six orthogonal views (front, rear, right, left, top, and bottom), spatially concatenated to form a 2×3 layout. The triplanar latent generation process is decomposed into two stages. We first diffuse hexaview latents using a modified and finetuned text-to-image U-Net (detailed in section 3.2.2). Then, we map these latents to our target triplanar representation, reusing the same diffusion U-Net for an additional inference step and a small layout converter (detailed in section 3.2.3). Computation-wise, this means we perform $N + 1$ U-Net inferences in total, N steps to obtain a multi-view representation of the object, and 1 additional U-Net forward pass to generate the corresponding mesh.

Unlike concurrent 3D asset generation approaches based

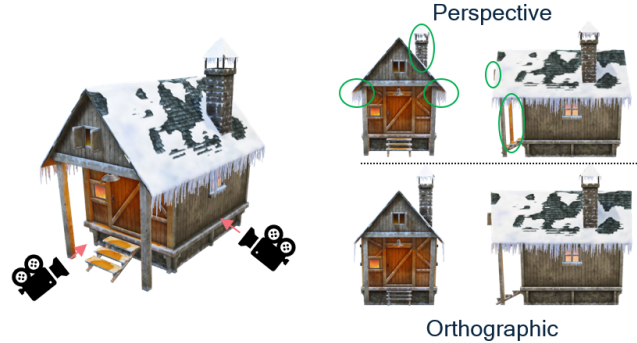


Figure 3. Perspective vs Orthographic views. Orthographic views are free from perspective distortions (highlighted in green), facilitating re-alignment to triplanar representations.

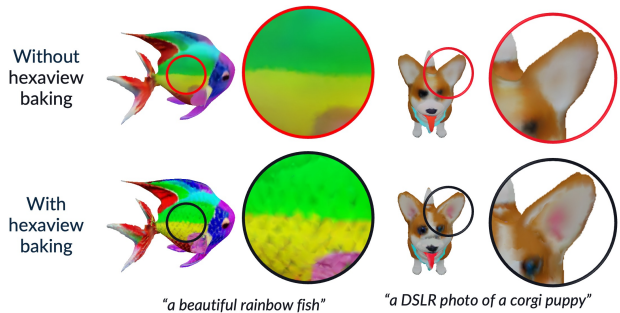


Figure 4. The orthographic hexaview prediction contains realistic details in the pixel space compared to the generated mesh. To significantly improve the visual feel of the final generated mesh, we “bake” the detailed hexaview prediction to the UV texture map (see Sec. 3.3).

on multi-view prediction [1, 40], a key and novel feature of our method is the use of orthographic projections*. As shown in Fig. 3, this form of parallel projection, commonly used in mechanical drawings of 3D parts, avoids perspective distortions, thereby guaranteeing pixel-accurate re-alignment of each orthogonal view to the corresponding plane in our target latent representation.

Another novel aspect of our approach is that the same 2D U-Net is trained to perform multi-view prediction and 3D asset generation simultaneously. To the best of our knowledge, this multi-task scenario has never been explored before. Interestingly, our results show that the same network can perform both tasks well and that the proposed hexaview guidance is in fact instrumental in unlocking high-quality 3D asset generation, offering a new technique to capitalize on the synthesis capabilities of large pre-trained text-to-image models.

* https://en.wikipedia.org/wiki/Orthographic_projection

3.2.2 U-Net architecture modifications

In our experiments, we adapt the U-Net architecture from StableDiffusion models, though we believe our method could be effectively applied to other text-to-image models as well. Fig. 2c illustrates the modifications we applied to the U-Net architecture, aimed at enhancing its suitability for the 3D domain:

Additional conditioning signals: Our first modification introduces two types of learnable encodings which we add to the timestep embeddings, providing a mechanism to modify the timestep-based modulations of convolutional and attention layers performed in the original U-Net. This modification draws inspiration from techniques like the camera embedding residuals in MVDream [40] or the domain switcher proposed in Wonder3D [21]. The first type of encodings is based on positional embeddings. These help in meeting the strict spatial alignment constraints imposed by the hexaview and triplane representations and can be thought as serving the same purpose as the 3D-aware convolutions in 3DGen [11]. The second type, domain encodings, involves learning distinct feature vectors for each phase of the generation process – one for the N hexaview diffusion steps (2D domain) and another for the final triplane mapping step (3D domain). This additional encoding allows our model to adjust its processing dynamically based on the current stage of the latent generation process.

“Make-it-3d” token: Another modification is the introduction of a special “Make-it-3d” token during the hexaview-to-triplane mapping step. The corresponding embedding vector is attended to via cross-attention layers and gives the U-Net component yet another mechanism to adapt its behavior specifically for triplane latent prediction.

3.2.3 Hexa-to-triplane Layout Converter

Following hexaview diffusion, we apply the U-Net for an additional inference step, using the 3D-specific conditioning techniques discussed in the previous section, and extract its penultimate features. We then map these features to the target triplane representation using a specialized module called hexa-to-triplane layout converter. As shown in Fig. 2d, our layout converter starts by re-orienting each view from the 2×3 input layout to align it with the corresponding plane from our 3D latent representation. This is achieved through a series of parameter-free operations, including slicing to isolate individual views, rotating and flipping to orient them correctly, and concatenating parallel views (i.e. top and bottom, left and right, front and back). The use of orthographic projections is advantageous here, as it guarantees pixel-accurate layout conversion and eliminates perspective distortions. A convolutional neural network (CNN)

then predicts the final triplane latents. In practice, the CNN’s main purpose is to adjust the number of channels to align with our independently-trained VAE. Our experiments indicate that the U-Net is effective in multi-tasking and predicting both hexaview latents and 3D-conditioned features that map well to the final triplane latents. Consequently, the additional CNN does not need to be very complex.

3.3. Texture baking for better visual appearance

In order to further enhance the visual appearance of the final mesh, we introduce a UV texture baking approach that leverages the six-sided orthographic views predicted during hexaview diffusion. Interestingly, these views often contain fine textural details that are missing in the VAE-decoded mesh. To address this, we adopt a post-processing procedure which “bakes” the intermediate hexaviews onto the decoded mesh, as illustrated in Fig. 2b. This procedure involves three steps:

1. **UV Mapping:** We employ an automatic UV unwrapping algorithm to create a UV mapping, making it possible to project a 2D texture onto the 3D mesh.
2. **Texture Initialization:** We then initialize our UV texture, mapping each texel to its corresponding 3D coordinate, sampling the corresponding triplane feature, and converting it to RGB using the Color MLP from our VAE decoder. While this step alone does not substantially enhance visual quality — even with increased texture resolution — it is crucial for areas not fully covered by the final hexaview baking step.
3. **Hexaview Baking:** We project pixels from the six (decoded) orthographic views onto the UV texture. In cases where multiple hexaview pixels correspond to the same texel, we average their values. This final step significantly enhances the visual quality of the mesh, as shown in Fig. 4.

While this texture baking procedure effectively addresses the limitations posed by the initial mesh decoding, further improvements in the VAE pipeline represent a promising avenue for future research. We believe that refining this component, such as potentially using higher-resolution latents, could alleviate some of the current bottlenecks, and we reserve this exploration for future work.

3.4. Implementation details

Training data. We train our models on 3D assets from the Objaverse dataset [8], complemented with automated captions generated by Cap3D [24]. Following findings from prior work [1, 11, 40], we filter out lower-quality assets from the original dataset, ultimately training our models on 86,784 curated objects. The selection criteria for these assets were based on factors such as geometric complexity



Figure 5. We compare “HexaGen3D” with other text-to-3D approaches: DreamFusion-SDv2.1 (DF) [32], TextMesh-SDv2.1 (TM) [43], MVDream-SDv2 (MV) [40], and Shap-E [13]. We use the threestudio [10] framework that implements the DF, TM, and MV approaches that leverages the StableDiffusion [36] text-to-image model. We use the text prompts from threestudio [10] based on DF.

and textural richness (more details can be found in the appendix).

In addition to 3D assets, we augment our training set with regular images while finetuning the latent diffusion model. The incorporation of 2D data helps to mitigate the limited amount of available 3D data and enhances the model’s generalization to unseen 3D objects. This form of multi-task regularization has been similarly employed in MVDream [40].

In terms of losses, we follow 3DGen and combine a mask silhouette loss, a depth loss, a laplacian smoothness loss and a KL divergence loss to supervise the geometry VAE, $L_{geometry} = \alpha L_{mask} + \phi L_{depth} + \lambda L_{smooth} - \gamma D_{KL}$, with $\alpha = 3$, $\phi = 10$, $\lambda = 0.01$, and $\gamma = 10^{-7}$, and use a sum of L1 and L2 losses to supervise the color VAE.

We train our VAE models for 15 epochs, using a batch size of 16, an initial learning rate of 3×10^{-5} and a cosine annealing schedule down to a minimum learning rate

of 10^{-6} . This takes roughly a week on 8 A100s.

Stage 2: Triplanar Latent Generation. Architecture-wise, we experimented with two pretrained StableDiffusion U-Net backbones: SD-v1.5 [36] and SD-XL [31]. The neural net used within our hexa-to-triplane layout converter is a two-layer convnet with SiLU activations and trained from scratch.

For the intermediate hexaview generation, we rasterize six 512×512 orthographic projections of the ground truth mesh, downscale them to 256×256 , and encode these images using the VAE encoder from the corresponding Stable Diffusion model. The resulting 32×32 latents are then re-organized into a 2×3 layout of size 64×96 . For 2D regularization, we use high-res images which we downsize to 256×256 , matching the resolution of individual views within our hexaview representation. Considering that StableDiffusion models often have difficulties with predicting

Method	Latency ↓ Single A100 GPU	CLIP score ↑			User preference score ↑	
		CLIP L/14	CLIP B/16	CLIP B/32	Vis. qual.	Prompt fid.
MVDream-SDv2.1 [40]	≈ 194 mins	25.02	30.35	29.61	0.97	0.88
TextMesh-SDv2.1 [43]	≈ 23 mins	19.46	25.06	24.86	0.12	0.21
DreamFusion-SDv2.1 [32]	≈ 22 mins	23.76	28.91	28.96	0.50	0.52
Shape-E [13]	≈ 7 secs	19.52	24.33	24.70	0.17	0.13
HexaGen3D-SDv1.5	≈ 7 secs	24.02	28.84	28.55	0.51	0.49
HexaGen3D-SDXL	≈ 7 secs	24.98	29.58	28.97	0.73	0.77

Table 1. Quantitative comparison of HexaGen3D with other approaches on 67 prompts from the DreamFusion [32] prompts available in threestudio [10]. We report the inference time on a single A100, CLIP scores for three different CLIP models, as well as user preference scores based on two criteria, visual quality and prompt fidelity. The preference scores reported here are obtained by averaging the pair-wise preference rates from Fig. 6.

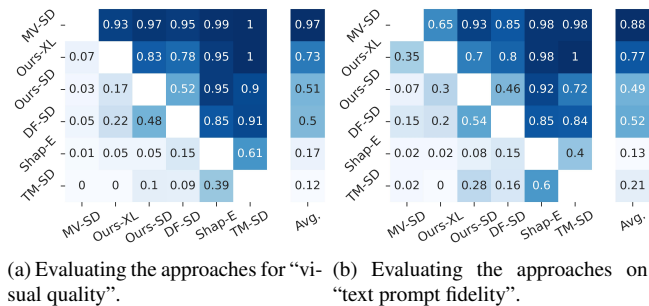


Figure 6. User study comparing all the text-to-3D approaches on (a) visual quality and (b) text prompt fidelity. Each cell indicates the user preference score (%) for an approach (row) over another (column). The approaches are: MVDream-SDv2.1 (MV-SD), DreamFusion-SDv2.1 (DF-SD), Shape-E, TextMesh-SDv2.1 (TM-SD), HexaGen3D-SDv1.5 (Ours-SD), and HexaGen3D-SDXL (Ours-XL).

plain white backgrounds [1], we add random colored backgrounds to the hexaviews. This addition does not impact triplanar latent generation, as the model effectively learns to disregard the background color in this context.

During training, we effectively optimize the model to solve three tasks simultaneously: hexaview latent generation, hexaview-to-triplane mapping and image latent generation (for regularization). We achieve this using gradient accumulation, aggregating gradients from all three tasks. We use a batch of 192 hexaviews for the hexaview diffusion and hexaview-to-triplanar mapping tasks, and a batch of 32 regular images for 2D regularization. We down-weight the diffusion loss coming from the 2D regularization batches by a factor 0.25. We train our latent generative models for 50,000 iterations using a learning rate of 3×10^{-5} . This takes roughly 4 days on 8 A100s.

Baselines We select a range of recent text-to-3D approaches for comparison with HexaGen3D, including a feedforward approach, Shap-E [13], and three SDS-based

Method	CLIP score ↑ CLIP L/14
(A1) HexaGen3D-SDv1.5	24.02
(A2) No Weight Sharing	23.43
(A3) No Hexaview Baking	21.85
(A4) No Hexaview Prediction	18.47
(B1) HexaGen3D-SDXL	24.98
(B2) No Weight Sharing	24.97
(B3) No Hexaview Baking	23.59

Table 2. We quantitatively compare different design choices in our HexaGen3D model and provide more detailed descriptions in section 4.2.

approaches, DreamFusion [32], TextMesh [43], and MVDream [40]. While we use the official implementation of Shap-E[†] and MVDream[‡], we leverage the DreamFusion and TextMesh implementations available within the three-studio framework [10], which include some notable deviations from their original papers. Specifically, our DreamFusion setup uses the open-source StableDiffusion v2.1 as the guidance model instead of Imagen [37], and a hash grid [28] as the 3D representation, diverging from MipNerf360 [2]. TextMesh similarly utilizes StableDiffusion v2.1 for guidance, with NeuS [44] replacing VolSDF [47] for the 3D signed distance field representation.

4. Experiments

As illustrated in Fig. 1, HexaGen3D generates high-quality textured meshes from a wide array of textual prompts, including complex prompts that involve unlikely combinations of objects, diverse styles or unique material properties. In Section 4.1, we compare HexaGen3D with existing methods, and Section 4.2 details our ablation study results.

[†]<https://github.com/openai/shap-e>

[‡]<https://github.com/bytedance/MVDream-threestudio>

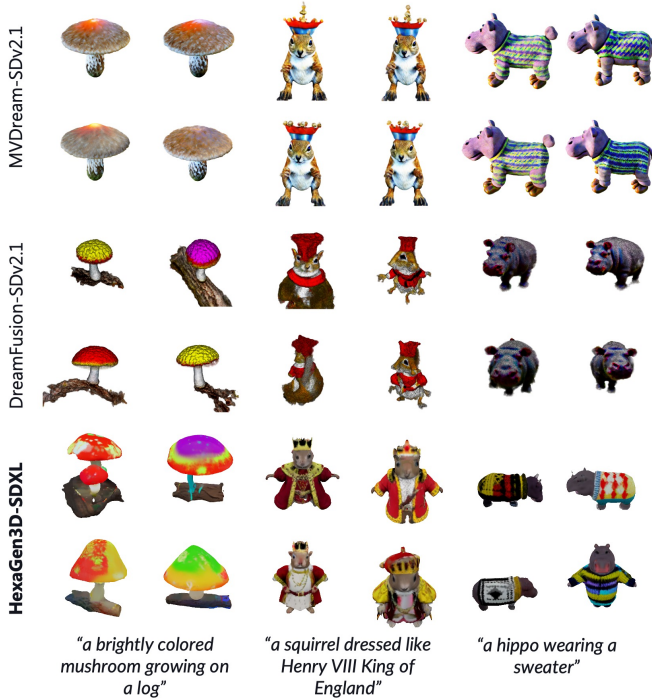


Figure 7. We show four (4) generations for each text prompt to demonstrate HexaGen3D generates more diverse 3D objects compared to the baseline MVDream-SDv2.1 and DreamFusion-SDv2.1 text-to-3D models.

4.1. Comparison against existing methods

Figure 5 shows a comparison of HexaGen3D against Shap-E [13], DreamFusion [32], TextMesh [43], and MVDream [40]. Our approach demonstrates superior performance in most aspects, notably offering significantly faster run times. While MVDream excels in producing higher-quality meshes, the extensive generation time hinders its practicality, as this baseline takes up to 3 hours to create an object on an NVIDIA A100 GPU — a process $1600\times$ slower than HexaGen3D, which accomplishes this in merely 7 seconds. Furthermore, MVDream exhibits limitations in terms of diversity, often leading to similar outputs across seeds. This point is illustrated in Fig. 7, where we show 4 generations for the same prompt, varying the seed, emphasizing the advantage of HexaGen3D in generating more diverse meshes.

In our quantitative comparison (Tab. 1), HexaGen3D, with variants based on SD v1.5 and SDXL, excels in mesh quality and prompt fidelity against these baselines, significantly outperforming Shape-E, the only other solution that can compete with HexaGen3D in terms of speed. Despite using an earlier version of StableDiffusion, our user studies and CLIP score evaluations indicate that HexaGen3D-SDv1.5 performs roughly on par with DreamFusion while

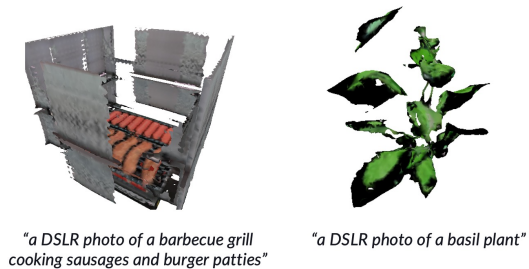


Figure 8. The generated 3D objects can contain minor limitations in terms of box artifacts, and intricate or thin mesh structures.

being $180\times$ faster. Switching to an SDXL backbone boosts our results significantly without impacting latency much. HexaGen3D-SDXL reaches a preference rate of 78% over DreamFusion (see Fig. 6) and an average prompt fidelity preference score of 0.77, narrowing the gap with MVDream’s score of 0.88 on this metric.

4.2. Ablation studies

We comprehensively validate some of our design choices through ablation studies in Table 2. Key findings can be summarized as follows:

- **Multi-tasking multi-view and 3D generation is beneficial.** We find it interesting that the same U-Net can perform both hexaview diffusion and hexaview-to-triplanar mapping with reasonable accuracy. In rows A2 and B2, we study how utilizing two distinct U-Nets (same architecture, separate weights) for these two tasks affects performance. Interestingly, using two separate networks leads to a noticeable performance drop with SDv1.5 (A2). With SD-XL (B2), removing weight sharing does not make much of a difference — but has the disadvantage of roughly doubling the model size and memory footprint.
- **Hexaview baking provides a significant quality boost.** Removing the finer textural details produced by our baking procedure translates into significantly lower CLIP scores, both with SDv1.5 (A3) or SDXL (B3).
- **Hexaview guidance is a necessary regularization.** Training the same model to directly denoise triplanar latents similar to 3DGen [11], without hexaview guidance (A4), leads to significantly worsened performance, illustrating the importance of using six-sided multi-view prediction as a surrogate task to steer the model toward triplanar latent generation.

5. Discussion

Our results demonstrate that existing text-to-image models can be directly adapted to 3D asset generation with only minor modifications and minimal fine-tuning data. To facilitate this knowledge transfer, we introduce orthographic hexaview guidance, a surrogate task designed specifically to steer the 2D capabilities of existing text-to-image models toward 3D synthesis. This task, which amounts to predicting six-sided orthographic projections, can be thought of as a form of multi-task regularization. Additionally, we present simple yet effective architectural modifications that better fit existing 2D diffusion architectures for 3D generation. We show the effectiveness of our approach through extensive experimental results and believe these techniques are widely applicable to various text-to-image models. Notably, our approach scales well to larger pre-trained text-to-image models, with the SDXL variant significantly outperforming its SDv1.5 counterpart, both in terms of mesh quality and prompt fidelity. This scalability highlights HexaGen3D’s potential in a context where 3D data is scarce.

While relatively rare, 3D objects generated by HexaGen3D occasionally contain artifacts such as a box scaffolding enclosing the 3D object as shown in Fig. 8 (left). This usually happens when the hexaview diffusion process generates inconsistent non-uniform backgrounds, leaving no choice but to add “walls” around the main object during triplanar latent generation to resolve these inconsistencies. Additionally, as observed in many other 3D mesh reconstruction techniques, generating 3D objects with intricate or thin structures is notoriously challenging — see Fig. 8 (right). Looking forward, exploring to what extent these issues could be resolved with more 3D data [7] would be interesting. Enhancing the VAE pipeline, which we mostly kept unchanged in this work compared to the original implementation proposed in 3DGen [11], present another exciting avenue for future research.

In conclusion, we believe HexaGen3D stands out as an innovative and practical solution in the field of 3D asset generation, offering a fast and efficient alternative to the current generation methods. HexaGen3D generates high-quality and diverse textured meshes in 7 seconds on an NVIDIA A100 GPU, making it orders of magnitude faster than existing approaches based on per-sample optimization. Leveraging models pre-trained on large-scale image datasets, HexaGen3D can handle a broad range of textual prompts, including objects or object compositions unseen during finetuning (see supplementary materials for more results, including generations from MS-COCO captions). Furthermore, HexaGen3D generates diverse meshes across different seeds, a significant advantage over SDS-based approaches like DreamFusion or MVDream. We believe these attributes make HexaGen3D a pioneering tool in the rapidly evolving domain of 3D content creation.

References

- [1] Anonymous. Instant3d: Fast text-to-3d with sparse-view generation and large reconstruction model. Under Review, 2023. 2, 4, 5, 7
- [2] Jonathan T Barron, Ben Mildenhall, Dor Verbin, Pratul P Srinivasan, and Peter Hedman. Mip-nerf 360: Unbounded anti-aliased neural radiance fields. In Proceedings of the IEEE/CVF Conference on Computer Vision and Pattern Recognition, pages 5470–5479, 2022. 7
- [3] Tianshi Cao, Karsten Kreis, Sanja Fidler, Nicholas Sharp, and Kangxue Yin. Textfusion: Synthesizing 3d textures with text-guided image diffusion models. In Proceedings of the IEEE/CVF International Conference on Computer Vision, pages 4169–4181, 2023. 3
- [4] Eric R Chan, Koki Nagano, Matthew A Chan, Alexander W Bergman, Jeong Joon Park, Axel Levy, Miika Aittala, Shalini De Mello, Tero Karras, and Gordon Wetzstein. Generative novel view synthesis with 3d-aware diffusion models. arXiv preprint arXiv:2304.02602, 2023. 2
- [5] Dave Zhenyu Chen, Yawar Siddiqui, Hsin-Ying Lee, Sergey Tulyakov, and Matthias Nießner. Text2tex: Text-driven texture synthesis via diffusion models. arXiv preprint arXiv:2303.11396, 2023. 3
- [6] Hansheng Chen, Jiatao Gu, Anpei Chen, Wei Tian, Zhuowen Tu, Lingjie Liu, and Hao Su. Single-stage diffusion nerf: A unified approach to 3d generation and reconstruction. arXiv preprint arXiv:2304.06714, 2023. 2
- [7] Matt Deitke, Ruoshi Liu, Matthew Wallingford, Huong Ngo, Oscar Michel, Aditya Kusupati, Alan Fan, Christian Laforte, Vikram Voleti, Samir Yitzhak Gadre, et al. Objaverse-xl: A universe of 10m+ 3d objects. arXiv preprint arXiv:2307.05663, 2023. 9
- [8] Matt Deitke, Dustin Schwenk, Jordi Salvador, Luca Weihs, Oscar Michel, Eli VanderBilt, Ludwig Schmidt, Kiana Ehsani, Aniruddha Kembhavi, and Ali Farhadi. Objaverse: A universe of annotated 3d objects. In Proceedings of the IEEE/CVF Conference on Computer Vision and Pattern Recognition, pages 13142–13153, 2023. 5
- [9] Jiatao Gu, Alex Trevithick, Kai-En Lin, Joshua M Susskind, Christian Theobalt, Lingjie Liu, and Ravi Ramamoorthi. Nerfdiff: Single-image view synthesis with nerf-guided distillation from 3d-aware diffusion. In International Conference on Machine Learning, pages 11808–11826. PMLR, 2023. 2
- [10] Yuan-Chen Guo, Ying-Tian Liu, Ruizhi Shao, Christian Laforte, Vikram Voleti, Guan Luo, Chia-Hao Chen, Zi-Xin Zou, Chen Wang, Yan-Pei Cao, and Song-Hai Zhang. threestudio: A unified framework for 3d content generation. <https://github.com/threestudio-project/threestudio>, 2023. 6, 7
- [11] Anchit Gupta, Wenhan Xiong, Yixin Nie, Ian Jones, and Barlas Oğuz. 3dgen: Triplane latent diffusion for textured mesh generation. arXiv preprint arXiv:2303.05371, 2023. 2, 3, 4, 5, 8, 9
- [12] Jonathan Ho, Ajay Jain, and Pieter Abbeel. Denoising diffusion probabilistic models. Advances in neural information processing systems, 33:6840–6851, 2020. 2

- [13] Heewoo Jun and Alex Nichol. Shap-e: Generating conditional 3d implicit functions. [arXiv preprint arXiv:2305.02463](#), 2023. [2](#), [4](#), [6](#), [7](#), [8](#)
- [14] Minguk Kang, Jun-Yan Zhu, Richard Zhang, Jaesik Park, Eli Shechtman, Sylvain Paris, and Taesung Park. Scaling up gans for text-to-image synthesis. In [Proceedings of the IEEE/CVF Conference on Computer Vision and Pattern Recognition](#), pages 10124–10134, 2023. [2](#)
- [15] Seung Wook Kim, Bradley Brown, Kangxue Yin, Karsten Kreis, Katja Schwarz, Daiqing Li, Robin Rombach, Antonio Torralba, and Sanja Fidler. Neuralfield-ldm: Scene generation with hierarchical latent diffusion models. In [Proceedings of the IEEE/CVF Conference on Computer Vision and Pattern Recognition](#), pages 8496–8506, 2023. [2](#)
- [16] Diederik P Kingma, Max Welling, et al. An introduction to variational autoencoders. [Foundations and Trends® in Machine Learning](#), 12(4):307–392, 2019. [3](#)
- [17] Chen-Hsuan Lin, Jun Gao, Luming Tang, Towaki Takikawa, Xiaohui Zeng, Xun Huang, Karsten Kreis, Sanja Fidler, Ming-Yu Liu, and Tsung-Yi Lin. Magic3d: High-resolution text-to-3d content creation. In [Proceedings of the IEEE/CVF Conference on Computer Vision and Pattern Recognition](#), pages 300–309, 2023. [2](#), [3](#)
- [18] Minghua Liu, Chao Xu, Haian Jin, Linghao Chen, Zexiang Xu, Hao Su, et al. One-2-3-45: Any single image to 3d mesh in 45 seconds without per-shape optimization. [arXiv preprint arXiv:2306.16928](#), 2023. [2](#)
- [19] Ruoshi Liu, Rundi Wu, Basile Van Hoorick, Pavel Tokmakov, Sergey Zakharov, and Carl Vondrick. Zero-1-to-3: Zero-shot one image to 3d object, 2023. [2](#)
- [20] Yuan Liu, Cheng Lin, Zijiao Zeng, Xiaoxiao Long, Lingjie Liu, Taku Komura, and Wenping Wang. Syncdreamer: Generating multiview-consistent images from a single-view image. [arXiv preprint arXiv:2309.03453](#), 2023. [2](#)
- [21] Xiaoxiao Long, Yuan-Chen Guo, Cheng Lin, Yuan Liu, Zhiyang Dou, Lingjie Liu, Yuexin Ma, Song-Hai Zhang, Marc Habermann, Christian Theobalt, et al. Wonder3d: Single image to 3d using cross-domain diffusion. [arXiv preprint arXiv:2310.15008](#), 2023. [2](#), [5](#)
- [22] Jonathan Lorraine, Kevin Xie, Xiaohui Zeng, Chen-Hsuan Lin, Towaki Takikawa, Nicholas Sharp, Tsung-Yi Lin, Ming-Yu Liu, Sanja Fidler, and James Lucas. Att3d: Amortized text-to-3d object synthesis. [arXiv preprint arXiv:2306.07349](#), 2023. [2](#)
- [23] Shitong Luo and Wei Hu. Diffusion probabilistic models for 3d point cloud generation. In [Proceedings of the IEEE/CVF Conference on Computer Vision and Pattern Recognition](#), pages 2837–2845, 2021. [2](#)
- [24] Tiange Luo, Chris Rockwell, Honglak Lee, and Justin Johnson. Scalable 3d captioning with pretrained models. [arXiv preprint arXiv:2306.07279](#), 2023. [5](#)
- [25] Yiwei Ma, Xiaoqing Zhang, Xiaoshuai Sun, Jiayi Ji, Haowei Wang, Guannan Jiang, Weilin Zhuang, and Rongrong Ji. X-mesh: Towards fast and accurate text-driven 3d stylization via dynamic textual guidance. In [Proceedings of the IEEE/CVF International Conference on Computer Vision](#), pages 2749–2760, 2023. [3](#)
- [26] Gal Metzer, Elad Richardson, Or Patashnik, Raja Giryes, and Daniel Cohen-Or. Latent-nerf for shape-guided generation of 3d shapes and textures. In [Proceedings of the IEEE/CVF Conference on Computer Vision and Pattern Recognition](#), pages 12663–12673, 2023. [2](#)
- [27] Ben Mildenhall, Pratul P Srinivasan, Matthew Tancik, Jonathan T Barron, Ravi Ramamoorthi, and Ren Ng. Nerf: Representing scenes as neural radiance fields for view synthesis. [Communications of the ACM](#), 65(1):99–106, 2021. [2](#)
- [28] Thomas Müller, Alex Evans, Christoph Schied, and Alexander Keller. Instant neural graphics primitives with a multiresolution hash encoding. [ACM Transactions on Graphics \(ToG\)](#), 41(4):1–15, 2022. [7](#)
- [29] Alex Nichol, Heewoo Jun, Prafulla Dhariwal, Pamela Mishkin, and Mark Chen. Point-e: A system for generating 3d point clouds from complex prompts. [arXiv preprint arXiv:2212.08751](#), 2022. [2](#)
- [30] Ryan Po, Wang Yifan, Vladislav Golyanik, Kfir Aberman, Jonathan T Barron, Amit H Bermano, Eric Ryan Chan, Tali Dekel, Aleksander Holynski, Angjoo Kanazawa, et al. State of the art on diffusion models for visual computing. [arXiv preprint arXiv:2310.07204](#), 2023. [2](#)
- [31] Dustin Podell, Zion English, Kyle Lacey, Andreas Blattmann, Tim Dockhorn, Jonas Müller, Joe Penna, and Robin Rombach. Sdxl: improving latent diffusion models for high-resolution image synthesis. [arXiv preprint arXiv:2307.01952](#), 2023. [2](#), [6](#)
- [32] Ben Poole, Ajay Jain, Jonathan T Barron, and Ben Mildenhall. Dreamfusion: Text-to-3d using 2d diffusion. [arXiv preprint arXiv:2209.14988](#), 2022. [2](#), [3](#), [6](#), [7](#), [8](#)
- [33] Charles R. Qi, Hao Su, Kaichun Mo, and Leonidas J. Guibas. Pointnet: Deep learning on point sets for 3d classification and segmentation. In [Proceedings of the IEEE Conference on Computer Vision and Pattern Recognition \(CVPR\)](#), July 2017. [3](#)
- [34] Aditya Ramesh, Mikhail Pavlov, Gabriel Goh, Scott Gray, Chelsea Voss, Alec Radford, Mark Chen, and Ilya Sutskever. Zero-shot text-to-image generation. In [International Conference on Machine Learning](#), pages 8821–8831. PMLR, 2021. [2](#)
- [35] Elad Richardson, Gal Metzer, Yuval Alaluf, Raja Giryes, and Daniel Cohen-Or. Texture: Text-guided texturing of 3d shapes. [arXiv preprint arXiv:2302.01721](#), 2023. [3](#)
- [36] Robin Rombach, Andreas Blattmann, Dominik Lorenz, Patrick Esser, and Björn Ommer. High-resolution image synthesis with latent diffusion models. In [Proceedings of the IEEE/CVF conference on computer vision and pattern recognition](#), pages 10684–10695, 2022. [2](#), [3](#), [4](#), [6](#)
- [37] Chitwan Saharia, William Chan, Saurabh Saxena, Lala Li, Jay Whang, Emily L Denton, Kamyar Ghasemipour, Raphael Gontijo Lopes, Burcu Karagol Ayan, Tim Salimans, et al. Photorealistic text-to-image diffusion models with deep language understanding. [Advances in Neural Information Processing Systems](#), 35:36479–36494, 2022. [2](#), [7](#)
- [38] Christoph Schuhmann, Romain Beaumont, Richard Vencu, Cade Gordon, Ross Wightman, Mehdi Cherti, Theo

- Coombes, Aarush Katta, Clayton Mullis, Mitchell Wortsman, et al. Laion-5b: An open large-scale dataset for training next generation image-text models. *Advances in Neural Information Processing Systems*, 35:25278–25294, 2022. 2
- [39] Tianchang Shen, Jun Gao, Kangxue Yin, Ming-Yu Liu, and Sanja Fidler. Deep marching tetrahedra: a hybrid representation for high-resolution 3d shape synthesis. *Advances in Neural Information Processing Systems*, 34:6087–6101, 2021. 3
- [40] Yichun Shi, Peng Wang, Jianglong Ye, Mai Long, Kejie Li, and Xiao Yang. Mvdream: Multi-view diffusion for 3d generation. *arXiv preprint arXiv:2308.16512*, 2023. 2, 4, 5, 6, 7, 8
- [41] J Ryan Shue, Eric Ryan Chan, Ryan Po, Zachary Ankner, Jiajun Wu, and Gordon Wetzstein. 3d neural field generation using triplane diffusion. In *Proceedings of the IEEE/CVF Conference on Computer Vision and Pattern Recognition*, pages 20875–20886, 2023. 2
- [42] Junshu Tang, Tengfei Wang, Bo Zhang, Ting Zhang, Ran Yi, Lizhuang Ma, and Dong Chen. Make-it-3d: High-fidelity 3d creation from a single image with diffusion prior. *arXiv preprint arXiv:2303.14184*, 2023. 2
- [43] Christina Tsalicoglou, Fabian Manhardt, Alessio Tonioni, Michael Niemeyer, and Federico Tombari. Textmesh: Generation of realistic 3d meshes from text prompts. *arXiv preprint arXiv:2304.12439*, 2023. 2, 6, 7, 8
- [44] Peng Wang, Lingjie Liu, Yuan Liu, Christian Theobalt, Taku Komura, and Wenping Wang. Neus: Learning neural implicit surfaces by volume rendering for multi-view reconstruction. *arXiv preprint arXiv:2106.10689*, 2021. 7
- [45] Tengfei Wang, Bo Zhang, Ting Zhang, Shuyang Gu, Jianmin Bao, Tadas Baltrusaitis, Jingjing Shen, Dong Chen, Fang Wen, Qifeng Chen, et al. Rodin: A generative model for sculpting 3d digital avatars using diffusion. In *Proceedings of the IEEE/CVF Conference on Computer Vision and Pattern Recognition*, pages 4563–4573, 2023. 4
- [46] Daniel Watson, William Chan, Ricardo Martin-Brualla, Jonathan Ho, Andrea Tagliasacchi, and Mohammad Norouzi. Novel view synthesis with diffusion models. *arXiv preprint arXiv:2210.04628*, 2022. 2
- [47] Lior Yariv, Jiatao Gu, Yoni Kasten, and Yaron Lipman. Volume rendering of neural implicit surfaces. *Advances in Neural Information Processing Systems*, 34:4805–4815, 2021. 7
- [48] Jiahui Yu, Yuanzhong Xu, Jing Yu Koh, Thang Luong, Gunjan Baid, Zirui Wang, Vijay Vasudevan, Alexander Ku, Yinfei Yang, Burcu Karagol Ayan, et al. Scaling autoregressive models for content-rich text-to-image generation. *arXiv preprint arXiv:2206.10789*, 2(3):5, 2022. 2
- [49] Biao Zhang, Jiapeng Tang, Matthias Niessner, and Peter Wonka. 3dshape2vecset: A 3d shape representation for neural fields and generative diffusion models. *arXiv preprint arXiv:2301.11445*, 2023. 2
- [50] Zibo Zhao, Wen Liu, Xin Chen, Xianfang Zeng, Rui Wang, Pei Cheng, Bin Fu, Tao Chen, Gang Yu, and Shenghua Gao. Michelangelo: Conditional 3d shape generation based on shape-image-text aligned latent representation. *arXiv preprint arXiv:2306.17115*, 2023. 2
- [51] Zhizhuo Zhou and Shubham Tulsiani. Sparsefusion: Distilling view-conditioned diffusion for 3d reconstruction. In *Proceedings of the IEEE/CVF Conference on Computer Vision and Pattern Recognition*, pages 12588–12597, 2023. 2
- [52] Zi-Xin Zou, Weihao Cheng, Yan-Pei Cao, Shi-Sheng Huang, Ying Shan, and Song-Hai Zhang. Sparse3d: Distilling multiview-consistent diffusion for object reconstruction from sparse views. *arXiv preprint arXiv:2308.14078*, 2023. 3